IMPROVEMENT OF THE LAP SHEAR STRENGTH OF RESISTANCE-WELDED THERMOPLASTIC COMPOSITE JOINTS USING A SILANE SOL-GEL COATING ON THE STAINLESS-STEEL HEATING ELEMENT

V. Rohart[1], M. Dubé[1*] and L. Laberge Lebel[2]

[1] Department of Mechanical Engineering, École de technologie supérieure, Montréal, Canada
[2] Department of Mechanical Engineering, Polytechnique Montréal, Montréal, Canada
*Corresponding author (martine.dube@etsmtl.ca)

Keywords: Thermoplastic composites, Resistance welding, Silane coating

ABSTRACT

Resistance welding of thermoplastic composites involves leaving a heating element, often in the form of a stainless-steel mesh, at the joint interface following the welding operation. Thermoplastic matrices, including polyphenylene sulfide (PPS), typically have low affinity with the stainless steel, preventing any adhesion between the polymer and the mesh. In this paper, we show the possibility of increasing the mechanical performance of resistance-welded carbon fibre/PPS (CF/PPS) joints through an improvement of the adhesion between the steel and the PPS. The better adhesion is created by applying an organosilane treatment on the mesh. To enable efficient grafting of the organosilane molecules, the steel was treated with a solution of sulfuric acid to remove the impure oxide layer and then oxidized at high temperature. This allowed the surface to be activated by increasing the concentration of oxides that could react with the hydrolyzed silane molecules. The grafting parameters under investigation are the solvent, silane hydrolysis time, silane concentration, reaction time and the rinsing of the mesh following the treatment. They were varied to obtain the best adhesion between the steel and the matrix of the composite and to understand the parameters affecting it. Measurement of the surface tension of the steel highlighted surface activation after acid treatment, mesh oxidation and silane coating. The results of the mechanical tests showed that a silane coating increased the lap shear strength of welded joints by 28%. A better adhesion of the matrix to the mesh after treatment was observed by electron microscopy. The matrix remains onto the steel surface after having mechanically tested the joint.

1 INTRODUCTION

One of the advantages of thermoplastic composites is their ability to be melted and reconsolidated several times [1]–[3]. It is thus possible to join them by welding. Welding thermoplastic composites consists of increasing the temperature at the interface of the two parts to be joined above the melting temperature of the matrix. The polymer chains then diffuse at the interface and the joint consolidates under the application of pressure during cooling. Among the various available welding processes, resistance welding was shown to be relatively fast, inexpensive and can be automated [4]. In this welding process, an electrically conductive and porous heating element (HE), often consisting of a stainless steel (SS) mesh, is placed between the parts to be welded. An electric current is introduced to the HE which heats up by joules effect and melts the matrix. Glass fibre thermoplastic composites usually show a failure occurring in the bulk composite adherends following mechanical testing. On the opposite, welded lap shear specimens made of stiff and strong unidirectional carbon fibre adherends show an interlaminar failure mode, with some damage at the weld interface. Observation of the fracture surfaces reveals a poor adhesion between the SS mesh and most thermoplastic polymers. It is thus believed that improving the HE/matrix adhesion would lead to higher joint performance when working with high performance carbon fibre composites.

Silanes are commonly used to improve the adhesion between organic and inorganic materials [5]. They are composed of organic and inorganic groups on the same molecule. The structure commonly used is: $YSi(OR)_3$ with -Y an organofunctional group such as an alkoxy, an epoxy, an active amine or a

thiol and -OR a hydrolysable alkoxy group. The silane molecules react with the oxides of the surfaces according to the mechanism shown in Figure 1: First, the alkoxy groups are hydrolyzed. The newly formed hydroxyl groups may then condense with those of neighbouring molecules forming oligomers. The oligomers then condense on the surface to be treated via hydrogen bonds. Finally, crosslinking is carried out thermally to form covalent bonds between the siloxane network and the surface [6]–[8]. For a variety of supports, the coating is efficient to improve its adhesion to polymers.
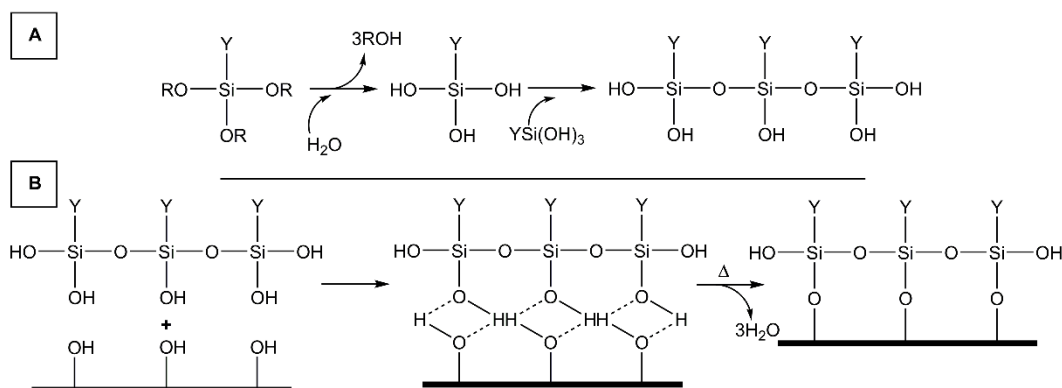
Figure 1: Silane hydrolysis mechanism [A] and condensation on an inorganic surface with crosslinking in temperature [B]. The metal surface represented as a bold line was previously treated by acid and oxidized to increase the hydroxyl groups (-OH) concentration

However, for every support-silane-polymer coupling, specific coating parameters must be used. For example, the silane hydrolyzed groups will condense on an oxide-rich metal surface, prompting the need to treat metals like stainless and galvanized steels with an oxidation process [9], [10]. Several studies showed that the mechanical performance of silane-treated SS bond to thermoplastic urethane was better if the SS was oxidized before the coating process [9]–[13], with an oxidation time varying between 5 and 100 minutes at 350°C. Five minutes was shown to only partially oxidize the surface while 100 minutes led to a homogeneous oxide layer however too thick and leading to low mechanical performance [12]–[14].

As is shown in Figure 1.a), the first step of the process is to hydrolyze the -OR groups into -OH groups. This step is done by stirring the silane – usually 1 to 2 vol% – in a solution of either water, ethanol or a mix of the two solvents. The silane is more soluble in ethanol which allows a faster grafting but can be hydrolyzed in water only. Solutions with 5 to 25 vol% of water in ethanol are frequently used [6], [8], [15]. The stirring time must be long enough to allow the complete hydrolysis of the alkoxy groups, and short enough to prevent any oligomerization i.e. silane molecules reacting with each other by condensation and creating agglomerates. Five to 60 minutes was considered acceptable [6], [8], [12], [15]. After the hydrolysis, the SS is immersed in the solution for five to 60 minutes [14], [16]. Finally, the crosslinking of the siloxane network can be carried out at room temperature for 24 hours [8] or at temperatures between 93°C and 110°C for five to 60 minutes [13]–[16].

The efficiency of the coating strongly depends on the parameters presented above: the time and solvent used for the silane grafting and the hydrolysis. This work aims at improving the adhesion between the SS HE and PPS by applying a silane coating on the HE to increase the LSS of resistance-welded CF/PPS joints. The coating as well as the failure modes of the joints were analyzed to understand the adhesion mechanisms and their effects on the LSS.

2 METHODOLOGY

2.1 Materials

The composite material consisted of unidirectional CF/PPS (TC1100, Ten Cate Advanced Composites). The laminates were composed of 16 UD plies stacked in a quasi-isotropic lay-up $[0/90/\pm45]_{2S}$. They were compression-moulded to form 254 x 254 mm² laminates in a hot press. The

temperature was increased to approximately 320°C under a 0.17 MPa contact pressure. The pressure was then increased to 0.7 MPa and held for 15 minutes. The material was then cooled down to room temperature under the application of pressure. The final thickness of the laminates was 3.3 mm. The laminates were then cut using a diamond saw in 101.6 mm X 25.4 mm coupons. The HE was a 304L SS plain weave mesh with an open gap width of 90 µm and a 40 µm wire diameter.

2.2 Coating process

First, the layer of oxides and impurities was removed from the SS meshes by corrosion with sulfuric acid (H_2SO_4) in aqueous solution at 60°C. Then the SS meshes were oxidized in an oven at 350°C for 30 minutes. The third step consisted in the (3-Aminopropyl)triethoxysilane (APTES) hydrolysis (the APTES solution was stirred at room temperature in a solvent) followed by the soaking of the HE in the solution at 60°C. For the last step, the HE were placed in an oven at 110°C for 15 minutes to cross-link the silanes to the steel. Each coating was applied on five HE meshes of 76 mm x 13 mm. The influence of five coating process factors on the LSS was studied. The nature of the solvent, the hydrolysis time, the APTES concentration, the grafting time and the washing before the last step. The parameters of every experiments are presented in Table 1. A total of six different treatments were conducted.

Sample	Corrosion	Oxydation	Solvent	Hydrolysis time (min)	APTES (vol%)	Grafting time (min)	Washing
UT							
A			EtOH			5	✗
B			H2O	60			
C	0,2M/30 min	350°C/30 min			1		✓
D			EtOH	0		60	
E				60			✗
F					2		

Table 1: Reaction parameters of all the treatments

2.4 Surface characterization

To assess the wettability of the steel after the different surface treatments, the water and the diiodomethane contact angles with the SS were measured. The measurements were made on 12.7×25.4 mm^2 treated or untreated 304 SS plates. A goniometer (VCA Optima, AST product inc.) was used to perform measurements with a liquid volume of 1 µL. The measurement was carried out exactly 10 seconds after the deposition to allow the drop to stabilize while avoiding evaporation of the solvent. For each surface, a minimum of three drops were deposited giving six contact angles, which were then averaged. The surface energy of the treated surfaces was calculated following the ASTM D7490-13 standard [17]. The water is a polar solvent and the diiodomethane is a nonpolar solvent. Their surface tension is known making it possible to calculate the surface energy of the support by substituting the contact angles of the two solvents in the equations of Owens-Wendt-Kaelble:

$$36,4(1 + \cos \theta_w) = \left[4,67\left(\gamma_s^d\right)^{1/2} + 7,14\left(\gamma_s^p\right)^{1/2}\right]$$
$$25,4(1 + \cos \theta_i) = \left[7,03\left(\gamma_s^d\right)^{1/2} + 1,14\left(\gamma_s^p\right)^{1/2}\right]$$

1

with θ_w and θ_i the contact angles of water and diiodomethane respectively. γ_s^d and γ_s^p are the dispersion and polar components of the support respectively (dyn/cm). Those equations are then solved to calculate γ_s^d and γ_s^p:

$$\gamma_s^p = \left[\frac{54,8(1 + \cos\theta_w) - 25,4(1 + \cos\theta_i)}{9,61}\right]^2$$
$$\gamma_s^d = \left[\frac{5,8(1 + \cos\theta_w) - 25,4(1 + \cos\theta_i)}{-6,28}\right]^2$$

2

The sum of the two components is the surface energy of the support. To obtain the standard deviation of the polar and disperse components, the standard deviations of the contact angles were implemented in the "Error Propagation Calculator" in which calculations are dependent on the Python module "Uncertainties: a Python package for calculations with uncertainties" by Eric O. Lebigot [18].

Observations were performed using a field emission scanning electron microscope (FE-SEM, SU-8230, Hitachi) equipped with an energy-dispersive X-ray (EDX) module on coated SS meshes that were scratched and cut to observe the silane coating on their surfaces. Lap shear specimens fracture surfaces following mechanical tests were also observed. EDX analysis was performed on the coated meshes, with chromium used to measure the surface activation by oxidation. Silicon was used to identify the silane coating.

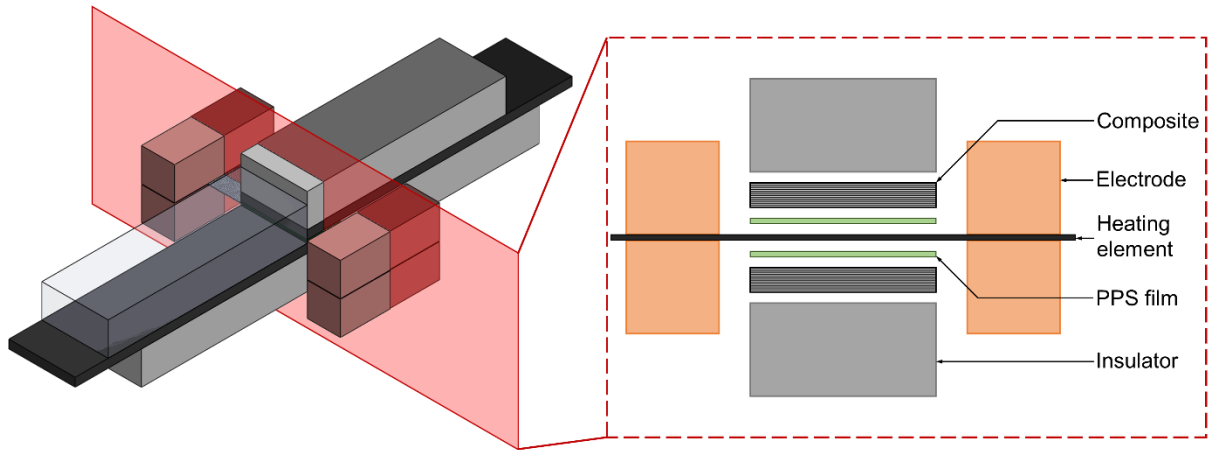## 2.5 Single lap shear welded samples

Figure 2: Schematic representation of the resistance welding setup

The composite joints were resistance-welded in a single lap shear configuration with an overlap width of 12.7 mm using the coated HE. The HE was cut 0.5 mm wider than the overlap to avoid side effects such as too low temperature at the ends of the overlap. A 80 μm thick PPS resin film was placed on both sides of the mesh to provide a resin-rich, void-free interface as shown in Figure 2 [19]. A constant pressure of 0.7 MPa was applied during the welding process. The joints were welded with a constant power of 110 W for 60 s and then allowed to cool down, under the application of pressure. The mechanical tests were based on the ASTM D1002 standard [20] and were conducted in a universal testing machine (Landmark, MTS) with a crosshead displacement speed of 1.3 mm/minute. Statistical analysis was performed on the LSS results with Minitab 18 software to know if the silane coating had a statistically significant influence on it.
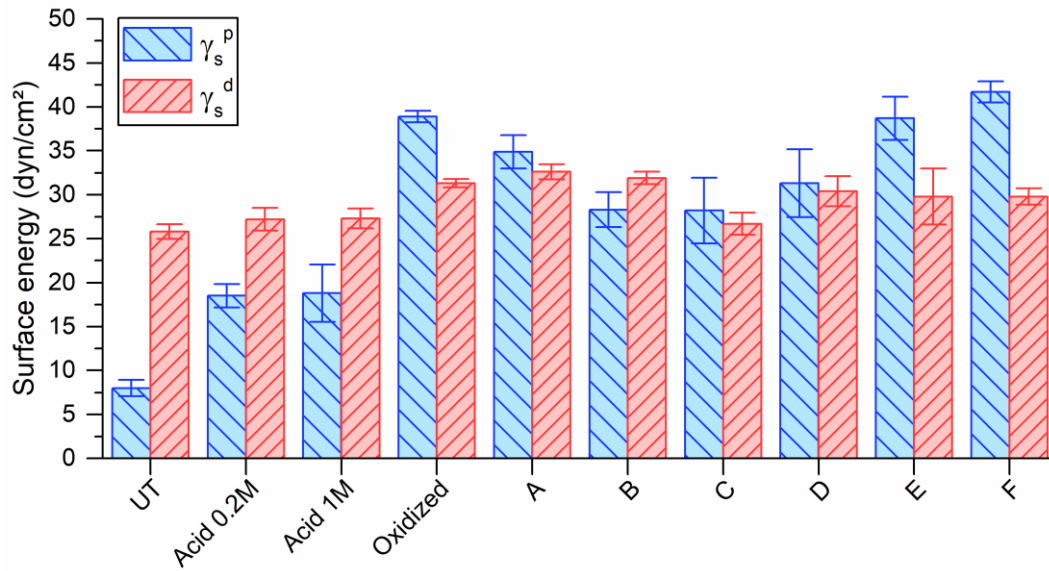
3 RESULTS

3.1 Surface tension

Figure 3: Disperse and polar components of the surface tension as a function of the surface treatments. For oxidized samples, a corrosion with 0.2M of H_2SO_4 was done prior to oxidation. Parameters of treatments A to F are provided in Table 1

The calculated polar and disperse components are presented in Figure 3. No change is seen in the disperse component γ_s^d of untreated (UT) and the two acid-treated samples (0.2M and 1M). Only the polar component is improved γ_s^p. The oxidation has an effect on γ_s^d mainly. Washing the mesh after the treatment seams to lower γ_s^p as $\gamma_s^p(A)$ and $\gamma_s^p(C)$ were lower than $\gamma_s^p(E)$. The highest γ_s^p was obtained with treatments E and F in which the mesh was not washed, a complete hydrolysis was done and the silanisation was done in EtOH solvent for 60 minutes. After silane coating, few changes were observed for γ_s^d. For the oxidized samples, γ_s^p was increased because of the formation of oxides with -OH terminations. Those groups are highly susceptible to form hydrogen bonds (that could condense with the silane -OH groups) as shown in Figure 1.

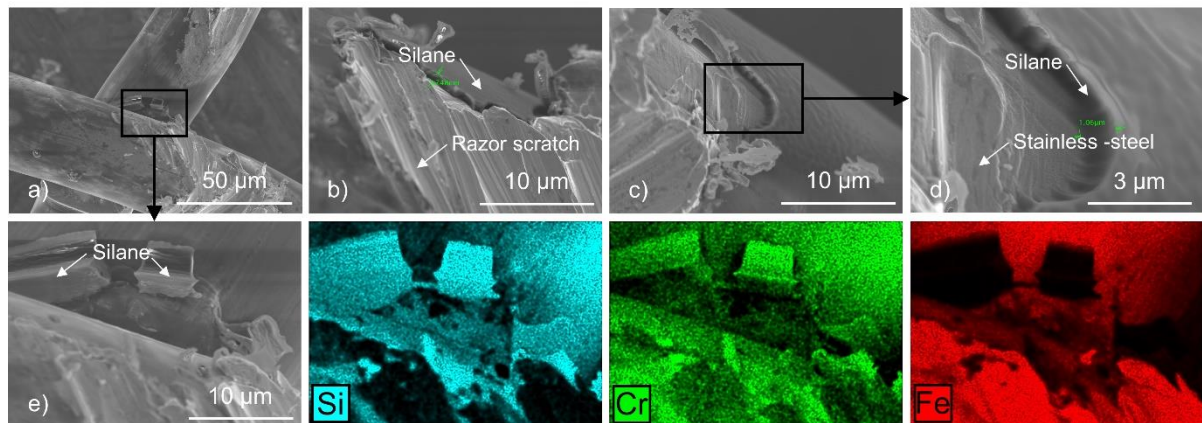## 3.3 Scanning electron microscopy

Figure 4: FE-SEM of the coated mesh with the treatment F. a) crossing between two SS wires; b) and c) Scratched wire with the visible coating; d) magnification of c) where the coating is on the right side and the scratch on the left; e) magnification of a) where the coating was partly removed. EDS analysis was made on e) for silicon (blue), chromium (green) and iron (red)

The FE-SEM observations of the SS mesh are shown in Figure 4. The mesh was scratched with a razor blade to allow observation of the coating and the steel. The coating is visible on the mesh in Figure 4-b) where the scratched steel appears brighter on the bottom and the coating appears darker, smoother and blurrier on the top. In Figure 4-c) the scratch is located on the left and a magnification is shown in Figure 4-d). The coating is located on the right. The thickness of the coating was measured in images b) and d) between 750 and 1000 nm. Figure 4-a) shows the crossing between two wires with some silane accumulation between them visible in the magnification e). These agglomerates were the results of the silane coating being scratched off the HE mesh by the relative movement of two wires crossing each other at their junction. An EDS analysis performed on the agglomerates revealed that they contained silicon, which confirmed that they came from the silane coating. Chromium was also found in these agglomerates, coming from the oxides, but no iron was detected.

The oxide layer and the silane coating cannot be discerned. This indicates a good adhesion between them as no interface was visible between them.
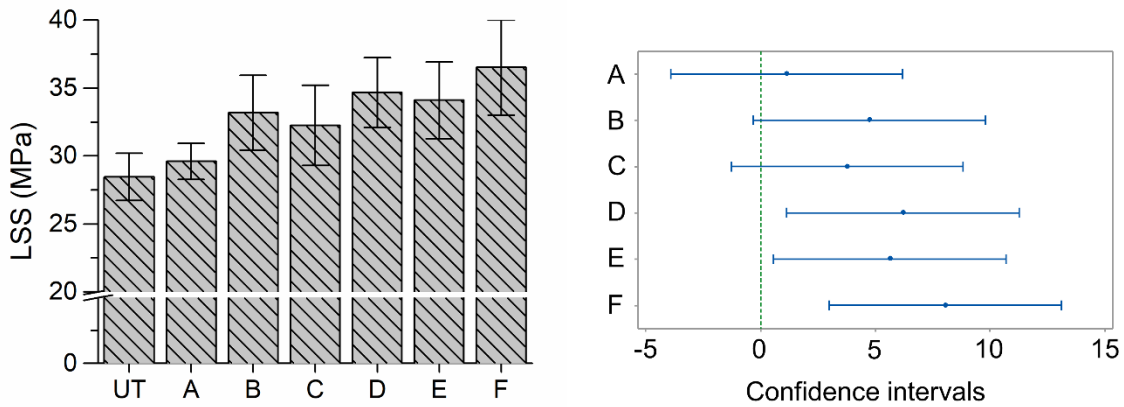
3.4 Mechanical tests

Figure 5: Apparent LSS of welded joints with silane-coated HE (on the left), the treatment parameters are listed in Table 1. The bars were cut between 4 and 26 MPa to improve the readability. Confidence intervals between the LSS of the joints welded with treated mesh and with untreated ones tested with Dunnett's method (on the right)

The LSS of the welded joints are shown in Figure 5 (left) for the various HE treatments. Treatment F improved the LSS the most with a 28% increase. An ANOVA test according to Dunnett's method [21] was used to determine whether any of the treatments produced LSS increase that is significantly different from the untreated joints. This method creates confidence intervals for differences between the average of each treatment and the average of a control group. Here the control group is the LSS of the joints with untreated mesh. The confidence intervals for the difference in mean LSS between the treatments and the untreated group are presented in Figure 5 (right). If an interval overlaps zero, then there is no significant difference between the mean LSS of the treatment under comparison and the mean LSS of the untreated samples. The confidence level was set to 95%. It appears that there were only three treatments that improved significantly the LSS of the welded joints: treatments D, E and F. All these treatments had in common a silanisation in ethanol for 60 minutes and a mesh that was not rinsed after silanisation. The only difference between treatments D and E was the hydrolysis that was done for 60 minutes for E and was not done for D. Both treatments led to similar results, which was explained by the long silanisation time. In studies where the silanisation was short [22][13], it was necessary to hydrolyse the silane prior to the reaction. In the current study, the 60 minutes of silanisation seemed enough to hydrolyse the silane and graft it on the SS.

3.5 Fractographic analysis

Figure 6 shows the fracture surfaces of a lap shear sample with untreated mesh and a lap shear sample welded with a treated mesh (parameters F). The untreated mesh is clearly visible as the main failure mode was cohesive between the SS and the PPS. SEM magnifications confirmed that there was no adhesion between the SS and the matrix. In Figure 6.g, some PPS residues are visible on the mesh. Greater magnifications showed the exposed mesh where the matrix was completely detached from the mesh (Figure 6.h). Figure 6.c shows the imprint of the mesh that was teared off the polymer. The treated mesh is less apparent in Figure 6.i. SEM observations showed that the mesh was almost entirely covered by the matrix (Figure 6.o). On large areas, the mesh was entirely covered by the matrix with imprints of the fibres seen in the PPS polymer (Figure 6.j and n). Failure occurred between the PPS and fibre rather than between the PPS and SS, showing a great improvement in the HE/PPS adhesion. We conclude that the silane coating was efficient in improving the adhesion between the SS and the PPS.
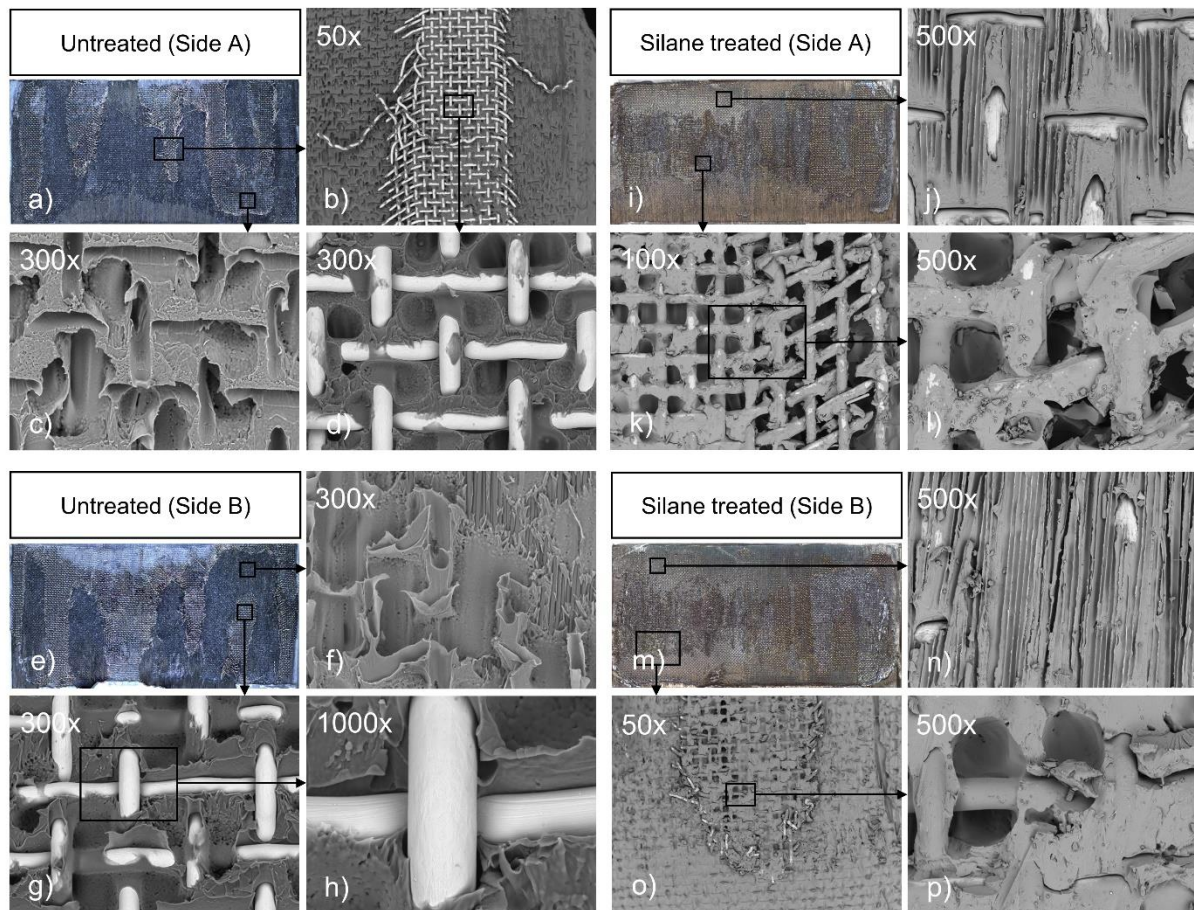

Figure 6: Fracture surfaces of welded joints after lap shear tests for untreated HE (a and e) and HE coated with the treatment F (i and m). SEM magnifications were made on a (b, c and d); e (f, g and h); i (j, k and l) and m (n, o and p) to observe the adhesion of the PPS on the SS

5 CONCLUSIONS

In this study, commonly used SS HE for resistance welding of thermoplastic composites were coated with a silane in order to improve the adhesion of the HE with the PPS polymer. A process in four steps was developed to clean and oxidized the SS, which enabled an efficient grafting of the silane molecule and the creation of a siloxane network. The impact on the LSS of five factors was studied. It was found that the grafting of the silane was more efficient with longer reaction time. The joints welded with coated HE led to an average LSS up to 36.5 MPa, an improvement of 28% compared to the specimens with untreated HE. The adhesion improvement was confirmed by visual and SEM observation of the

fractured surfaces of the joints. It was shown that the coating led to a much better adhesion between the HE and PPS. Contact angles turned out to be a good indicator to measure the efficiency of the corrosion and the oxidation steps in the coating process. The treatment leading to a SS surface with the highest polar energy was also the one with the best LSS.

ACKNOWLEDGEMENTS

REFERENCES

[1]   H. Li and K. Englund, "Recycling of carbon fiber-reinforced thermoplastic composite wastes from the aerospace industry," *J. Compos. Mater.*, vol. 51, no. 9, pp. 1265–1273, 2017.

[2]   N. Benoit, "Mechanical recycling of high density polyethylene / flax fiber composites Mechanical recycling of high density polyethylene / flax fiber composites," 2017.

[3]   M. Roux, C. Dransfeld, N. Eguémann, and L. Giger, "Processing and Recycling of a Thermoplastic Composite Fibre / Peek Aerospace Part," *16Th Eur. Conf. Compos. Mater.*, no. June, pp. 22–26, 2014.

[4]   I. Fernandez Villegas *et al.*, "Process and performance evaluation of ultrasonic , induction and resistance welding of advanced thermoplastic composites," *J. Thermoplast. Compos. Mater.*, vol. 26, no. 8, pp. 1007–1024, 2012.

[5]   M. Grujicic *et al.*, "An overview of the polymer-to-metal direct-adhesion hybrid technologies for load-bearing automotive components," *J. Mater. Process. Technol.*, vol. 197, no. 1–3, pp. 363–373, 2008.

[6]   Gelest Inc., "SILANE COUPLING AGENTS," 2014.

[7]   D. Corning, "A guide to silane solutions from Dow Corning," *USA Dow Corning. Retrieved July*, 2005.

[8]   S. I. L. Ane and A. G. U. I. De, "Silane coupling agent guide," *UCT*.

[9]   S. Bera, T. K. Rout, G. Udayabhanu, and R. Narayan, "Water-based & eco-friendly epoxy-silane hybrid coating for enhanced corrosion protection & adhesion on galvanized steel," *Prog. Org. Coatings*, vol. 101, pp. 24–44, 2016.

[10]   A. Foerster *et al.*, "Stainless steel surface functionalization for immobilization of antibody fragments for cardiovascular applications," *J. Biomed. Mater. Res. - Part A*, vol. 104, no. 4, pp. 821–832, 2016.

[11]   Honkanen, "Characterisation of stainless steel surfaces - modified in air at 350°C," *Surf. Eng.*, vol. 27, no. 5, 2011.

[12]   M. Honkanen *et al.*, "Characterization of silane layers on modified stainless steel surfaces and related stainless steel-plastic hybrids," *Appl. Surf. Sci.*, vol. 257, no. 22, pp. 9335–9346, 2011.

[13]   M. Hoikkanen, M. Honkanen, M. Vippola, T. Lepistö, and J. Vuorinen, "Effect of silane treatment parameters on the silane layer formation and bonding to thermoplastic urethane," *Prog. Org. Coatings*, vol. 72, no. 4, pp. 716–723, 2011.

[14]   M. Honkanen, M. Hoikkanen, M. Vippola, J. Vuorinen, and T. Lepistö, "Metal–Plastic Adhesion in Injection-Molded Hybrids," *J. Adhes. Sci. Technol.*, vol. 23, no. 13–14, pp. 1747–1761, Jan. 2009.

[15]   P. Jussila, H. Ali-L Öytty, K. Lahtonen, M. Hirsimäki, and M. Valden, "Effect of surface hydroxyl concentration on the bonding andmorphology of aminopropylsilane thin films on austenitic stainless steel," *Surf. Interface Anal.*, vol. 42, no. 3, pp. 157–164, 2010.

[16]   B. Golaz, V. Michaud, and J. A. E. Månson, "Photo-polymerized epoxy primer for adhesion improvement at thermoplastics/metallic wires interfaces," *Compos. Part A Appl. Sci. Manuf.*, vol. 48, no. 1, pp. 171–180, 2013.

[17]   ASTM D7490-13, "Standard D7490-13 Standard Test Method for Measurement of the Surface Tension of Solid Coatings, Substrates and Pigments using Contact Angle Measurements," *ASTM Int.*, pp. 1–5, 2013.

[18]   Eric O. LEBIGOT, "Uncertainties: a Python package for calculations with uncertainties." .

[19]   D. Stavrov and H. E. N. Bersee, "Resistance welding of thermoplastic composites-an overview," *Compos. Part A Appl. Sci. Manuf.*, 2005.

[20]   ASTM.D1002-05, "Standard Test Method for Apparent Shear Strength of Single-Lap-Joint Adhesively Bonded Metal Specimens by Tension Loading (Metal-to-Metal)," *ASTM Int.*, 2005.

[21]   C. W. Dunnett and A. C. Tamhane, "Multiple testing to establish superiority/equivalence of a new treatment compared with k standard treatments," *Stat. Med.*, vol. 16, no. 21, pp. 2489–2506, 1997.

[22]   M. Honkanen, M. Hoikkanen, M. Vippola, J. Vuorinen, and T. Lepistö, "Metal-plastic adhesion in injection-molded hybrids," *J. Adhes. Sci. Technol.*, vol. 23, no. 13–14, pp. 1747–1761, 2009.